

Comprehensive evaluation of chip interleaving effect on turbo-coded DS-SS in a Rayleigh fading channel with antenna diversity reception

Deepshikha Garg*[†] and Fumiyuki Adachi

Electrical and Communication Engineering, Graduate School of Engineering, Tohoku University, 05 Aza-Aoba, Aramaki, Aoba-ku, Sendai 980-8579, Japan

Summary

In this paper, we present a comprehensive performance evaluation of chip interleaving effect on turbo coded direct sequence spread spectrum (DS-SS) system in a frequency non-selective Rayleigh fading channel with antenna diversity reception. At the transmitter, chip interleaver scrambles the SF (spreading factor) chips associated with a data symbol and transforms the transmission channel into a highly time-selective or highly memoryless channel at the chip level. The use of chip interleaving is equivalent to using SF-antenna diversity reception with correlated fading among the branches and with reduced average received signal power per antenna by a factor of SF. We theoretically analyze how chip interleaving alters the received signal statistics. Then, the effect of the various parameters, *viz.* interleaver size, interleaving depth, information sequence length, spreading factor and the fading maximum Doppler frequency, are also evaluated. It is found that the bit error rate (BER) performance improves with increasing spreading factor and increasing frame length. Chip interleaving is found to be effective in the presence of receive antenna diversity as well. Copyright © 2005 John Wiley & Sons, Ltd.

KEY WORDS: chip interleaver; turbo codes; fading channel; direct sequence spread spectrum

1. Introduction

Recently, direct sequence code division multiple access (DS-CDMA) based on DS-spread spectrum (SS) has been adopted for the cellular mobile communications systems because of its high spectrum efficiency [1]. In DS-SS, the data-modulated symbol sequence to be transmitted is spread over a wideband channel by multiplying each data-modulated symbol by a spreading code (this is called spreading modulation); the resulting sequence is called a chip sequence. The chip sequence is then transmitted over the wireless chan-

nel. In DS-SS, rake combining [2] can be utilized in a frequency selective channel to attain multipath diversity for improving the transmission performance; however in a frequency non-selective fading channel rake combining effect cannot be expected. For such a channel, diversity techniques and channel coding are attractive. Channel coding has been effectively employed in the mobile communications systems for a long time [3].

Turbo codes [4] are efficient channel codes introduced in 1993 by Berrou et al. and found to give performance close to the Shannon capacity for very

*Correspondence to: Deepshikha Garg, Electrical and Communication Engineering, Graduate School of Engineering, Tohoku University, 05 Aza-Aoba, Aramaki, Aoba-ku, Sendai 980-8579, Japan.

[†]E-mail: deep@mobile.ecei.tohoku.ac.jp

long frame lengths in an additive white Gaussian noise (AWGN) channel. However in a fading environment, the bit error rate (BER) performance degrades drastically even with channel interleaving. This is because, although the fading channel can be memoryless with a conventional channel bit interleaving, the probability density function (pdf) of the received coded bit energy cannot be altered (it still has an exponential distribution in a Rayleigh fading channel). If the channel interleaver is designed to alter the pdf of the received signal bit energy so that the probability of low bit energy can be reduced, the resultant BER performance can be significantly improved compared to that with bit interleaving. Chip interleaving provides a way to improve the received signal statistics thereby improving turbo decoding performance. Time diversity in the form of chip interleaving has been proposed in Reference [5]. At the transmitter, chip interleaver scrambles the chips associated with a data-modulated symbol so that the channel gains experienced by neighboring chips are highly uncorrelated. By doing so, the resultant transmission channel can be transformed into a highly time-selective or highly memoryless channel. At the receiver side, the received chip sequence is first de-interleaved, and then despread. During the despreading operation, the fading effect is significantly reduced.

Other applications of chip interleaving in a multipath fading channel can be found in References [6,7]. Short spreading codes (their repetition length is equal to the spreading factor (SF)) are used. When an $M \times \text{SF}$ -chip block interleaving is used, where M represents the block length in symbol, no interference is produced between successive chips of the same data symbol but only from interleaved chips of other data symbols. Chip interleaving can replace the inter-chip interference (or inter-path interference) by the intersymbol interference. This facilitates the joint estimation of channel impulse responses associated with multiple users, without requiring training sequences [7]. If orthogonal spreading codes are used for multiple users, the use of chip interleaving converts a multi-user detection problem into a set of equivalent single-user equalization problem, i.e. multi-user-interference free reception is possible [7]. In Reference [8] also, chip interleaving is used to mitigate multi-access interference (MAI) in a multi-user environment without complicated multi-user detection. The analyses in Reference [8] show that more users can be accommodated with chip interleaved DS-CDMA than conventional DS-CDMA for the same BER. References [6–8] are not intended to reduce the variations in the

received signal bit energy by altering the fading statistics in the chip time level.

The fundamental chip interleaving idea was proposed in Reference [5]. This paper provides a comprehensive evaluation of how chip interleaving changes the received signal statistics for a frequency non-selective fading channel with antenna diversity reception. The frequency non-selective fading channel is the most severe channel for DS-SS systems, since rake combining effect cannot be expected. The improvement in the turbo decoding performance owing to the use of chip interleaving is also investigated and the effect of the various parameters, *viz.*, interleaver size, interleaving depth, information sequence length, spreading factor and the fading maximum Doppler frequency, are also evaluated. Single-user transmission is assumed because we want to focus on how the use of chip interleaving alters the pdf of the received signal bit energy and thus, improves the transmission performance.

The remainder of this paper is organized as follows. The transmission system model with chip interleaving is presented in Section 2. Then, in Section 3, we theoretically analyze the pdf of the received signal bit energy and the uncoded BER performance when a chip interleaver is used. In Section 4, we present the computer simulation results showing the improved BER performance with chip interleaving. The turbo coded BER performance achievable by the use of chip interleaving is also presented and the impact of various system parameters including the number of diversity antennas are discussed. Section 5 offers some conclusions and future work.

2. Transmission System Model with Chip Interleaving

Figure 1 shows the DS-CDMA transmission system model with chip interleaving.

2.1. Turbo Coding and Spreading

An information sequence $\{u_k; k = 0 \sim (K - 1)\}$ of length K is coded by a turbo encoder giving a binary sequence $\{v_n; n = 0 \sim (N - 1)\}$, where N is the coded sequence length (it is assumed that N is the punctured coded sequence length). This coded bit sequence is transformed into a data-modulated symbol sequence $\{d_n\}$. For channel estimation at the receiver, known pilot symbols are time-multiplexed with the data symbol sequence before spreading.

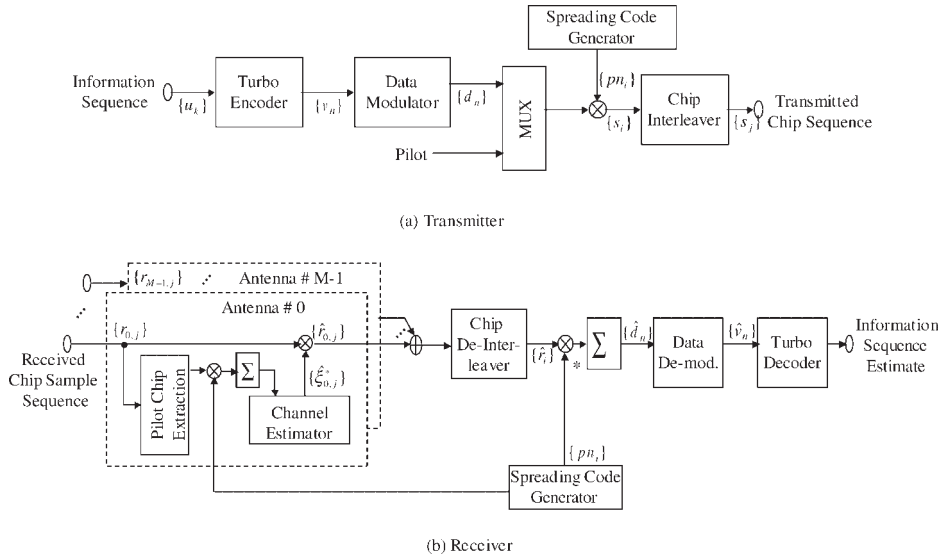


Fig. 1. Transmission system model with chip interleaving.

Spreading is implemented by multiplying the pilot-inserted binary phase shift keying (BPSK) symbol sequence, having symbol period T , with the long pseudo random (PN) sequence $\{pn_i\}$ having chip period T_c . The spread chip sequence $\{s_i\}$ to be transmitted can be expressed in the equivalent low-pass form as

$$s_i = \sqrt{2A}d_npn_i \quad (1)$$

where A is the average signal power and $n = \lfloor i/SF \rfloor$, with $SF = T/T_c$ being the spreading factor ($\lfloor a \rfloor$ denotes the largest integer smaller than or equal to a). Chip interleaver accepts blocks of chips and interleaves them giving the new spread sequence $\{s_j\}$, which is transmitted over the channel. As was mentioned previously, the idea is to distribute the chips belonging to a symbol as far as possible such that the channel gains on these chips are highly uncorrelated.

2.2. Chip Interleaver Structure and Pilot Insertion

Figure 2 illustrates the chip interleaver [5], which is a block interleaver with the number of rows equal to the number of symbols to be transmitted and the columns equal to SF . The chips are spread in time such that the fades experienced by the chips of a symbol have very small correlation. The chips falling in deep fades belong to different symbols. When chip interleaver is not used, N_p pilot symbols are inserted every N_d data symbols to assist in the channel estimation [9].

However, when chip interleaving is applied, pilot symbols must be time-multiplexed with data symbol sequence so that pilot chips appear periodically such that homogeneous channel estimation can be performed over the transmitted sequence before chip de-interleaving. The chip-interleaver structure shown in Figure 2 is an $[N(1 + N_p/N_d) \times SF]$ -chip block interleaver. With chip interleaver, $N_p \times SF$ pilot symbols are inserted every $N_d \times SF$ data symbols. The pilot and data symbols are spread and written in the chip interleaver row-wise and read out column-wise such that $(N_p \times SF)$ pilot chips appear every $(N_d \times SF)$ data

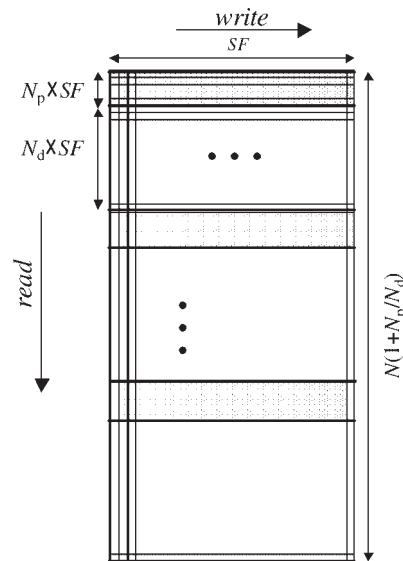


Fig. 2. Chip interleaver structure.

chips in the interleaved sequence. The resulting pilot-chip inserted sequence $\{s_j\}$ consists of $N \times \text{SF}(1 + N_p/N_d)$ chips and is transmitted via a propagation channel that is assumed to be a frequency non-selective Rayleigh fading channel.

2.3. Antenna Diversity Combining and Despreading

M receive antennas are assumed for diversity combining. The faded signal, corrupted by AWGN, received by each antenna is input to a chip-matched filter. Assuming ideal sampling timing, the output of the chip-matched filter for the m th antenna ($m = 0 \sim (M-1)$) is sampled at the chip rate, giving the received chip sample sequence $\{r_{m,j}\}$. Pilot chips are extracted, despread and manipulated for channel estimation before de-interleaving the data chip sequence. Using the channel estimate, coherent detection of the received spread signal is performed in a chip wise manner. The coherently detected chip sample sequence $\{\hat{r}_{m,j}\}$ is represented by

$$\hat{r}_{m,j} = r_{m,j} \hat{\xi}_{m,j}^* \quad (2)$$

where $\hat{\xi}_{m,j}$ is the estimated fading channel gain associated with the j th chip received by the m th antenna and $(.)^*$ represents the complex conjugate. The chips from M antennas are combined using the maximum ratio combining (MRC) [2] scheme and chip de-interleaving is performed. The chip de-interleaved sequence $\{\hat{r}_i\}$ after MRC is expressed as

$$\hat{r}_i = \sum_{m=0}^{M-1} \hat{r}_{m,i} p n_i \quad (3)$$

Despreading is performed after chip de-interleaving, i.e. the chip de-interleaved sequence is multiplied by the locally generated spreading sequence $\{p n_i\}$ and summed up over one BPSK symbol period T . Since the chips spread in time are combined, the pdf of the received signal bit energy is altered, but its average value remains the same. What is different from the bit interleaving is that chip interleaving alters the pdf of the received signal bit energy, while the bit interleaving does not. The theoretical analysis of how chip interleaving alters the pdf of the received signal bit energy is presented in Section 3. Despreading is carried out to obtain

$$\hat{d}_n = \sum_{i=n\text{SF}}^{(n+1)\text{SF}-1} \hat{r}_i \quad (4)$$

which is used for data demodulation followed by turbo decoding. Turbo decoding requires soft decision sample sequence corresponding to $\{\hat{v}_n\}$, which is denoted as $\{\hat{v}_n\}$ in this paper. Since the channel gains $\{\xi_{m,i}, i = n\text{SF} \sim (n+1)\text{SF} - 1\}$ are collected from widely spread time positions, they are nearly independent of each other, if the fading rate is not too slow due to the chip interleaving. Hence, as mentioned earlier, the probability of the signal bit being corrupted by the noise reduces, thereby improving the BER performance.

3. Theoretical Analysis

In the theoretical analysis, without loss of generality, BPSK modulation is assumed.

3.1. Data-Demodulator Output

The coherently detected chip sample sequence $\{\hat{r}_{m,i}\}$ can be represented as

$$\hat{r}_{m,i} = \left(\sqrt{2A} \xi_{m,i} d_n p n_i + n_{m,i} \right) \hat{\xi}_{m,i}^* \quad (5)$$

where $d_n = \pm 1$ for BPSK data modulation, $\xi_{m,i}$ is the complex fading channel gain associated with the i th chip received by the m th antenna (its estimate is denoted by $\hat{\xi}_{m,i}$ as in Equation (2)) and $\{n_{m,i}\}$ is the Gaussian random process with mean 0 and variance $2N_0/T_c$, N_0 is the AWGN single-sided power spectrum density. Assuming a Rayleigh fading channel, $\{\xi_{m,i}\}$ is a complex Gaussian process with mean 0 and variance 1. The soft decision sample sequence $\{\hat{v}_n\}$ obtained after MRC, chip de-interleaving, despreading and BPSK demodulation is given by

$$\begin{aligned} \hat{v}_n = \text{Re}[\hat{d}_n] &= \sqrt{2A} d_n \text{Re} \left(\sum_{m=0}^{M-1} \sum_{i=n\text{SF}}^{(n+1)\text{SF}-1} \xi_{m,i} \hat{\xi}_{m,i}^* \right) \\ &+ \text{Re} \left(\sum_{m=0}^{M-1} \sum_{i=n\text{SF}}^{(n+1)\text{SF}-1} n_{m,i} \hat{\xi}_{m,i}^* \right) \end{aligned} \quad (6)$$

where the first term represents the signal component and the second the noise component. The soft values are input to the turbo decoder.

3.2. Pdf of Received Signal Bit Energy

Without loss of generality, transmission of the 0th coded bit is considered. The instantaneous

signal-to-noise ratio (SNR) per bit after MRC, chip de-interleaving and despreading is given by, from Equation (6)

$$\text{SNR} = 2\gamma \quad (7)$$

where

$$\gamma = \left(\frac{\Gamma}{\text{SF}}\right) \frac{\left(\text{Re}\left(\sum_{m=0}^{M-1} \sum_{i=0}^{\text{SF}-1} \xi_{m,i} \hat{\xi}_{m,i}^*\right)\right)^2}{\sum_{m=0}^{M-1} \sum_{i=0}^{\text{SF}-1} |\hat{\xi}_{m,i}^*|^2} \quad (8)$$

is the instantaneous received SNR per bit, in which Γ is the average received energy per bit-to-AWGN power spectrum density ratio E_b/N_0 per antenna given by AT/N_0 . Assuming ideal channel estimation, i.e. $\hat{\xi}_{m,i} = \xi_{m,i}$, Equation (8) reduces to

$$\gamma = \sum_{m=0}^{M-1} \sum_{i=0}^{\text{SF}-1} \gamma_{m,i} \quad (9)$$

with

$$\begin{cases} \gamma_{m,i} = \bar{\gamma}_c |\xi_{m,i}|^2 \\ \bar{\gamma}_c = \frac{\Gamma}{\text{SF}} \end{cases} \quad (10)$$

where $\gamma_{m,i}$ is the instantaneous energy per chip-to-AWGN power spectrum density ratio E_c/N_0 of the m th antenna and $\bar{\gamma}_c$ is the average E_c/N_0 per antenna, which is assumed to be identical for all chips. It should be noted that when the pilot-assisted channel estimation is used, $\hat{\xi}_{m,i} \neq \xi_{m,i}$, and therefore, the SNR of Equation (7) becomes less than two times the instantaneous received E_b/N_0 . This means that the received signal energy cannot be fully utilized in BPSK data demodulation, thereby the achievable BER performance using the pilot-assisted channel estimation degrades compared to the ideal channel estimation case.

How chip interleaving alters the pdf shape of γ is discussed below assuming that $\{\xi_{m,i}\}$ are independent. Remember that the real and imaginary parts of $\xi_{m,i}$ are independent and identically distributed (i.i.d.) complex-valued Gaussian variables in the Rayleigh fading channel. Therefore, γ is χ^2 distributed with $2 \times$

$\text{SF} \times M$ degrees of freedom. The γ -pdf can be obtained as follows [2]:

$$p(\gamma) = \frac{1}{(\text{SF} \times M - 1)! \bar{\gamma}_c} \left(\frac{\gamma}{\bar{\gamma}_c}\right)^{\text{SF} \times M - 1} \exp\left(-\frac{\gamma}{\bar{\gamma}_c}\right) \quad (11)$$

which is equivalent to $\text{SF} \times M$ -branch MRC diversity reception with uncorrelated fading and $\bar{\gamma}_c$ being the average received E_c/N_0 per antenna. Thus, the deep fades in the channel can be effectively avoided. The fading nature experienced after despreading tends to disappear as a result of chip interleaving.

The theoretical pdf of γ/Γ obtained from Equation (11) is plotted with SF as a parameter in Figure 3 for no antenna diversity ($M = 1$). In this case, the use of chip interleaving is equivalent to using SF antenna diversity and the probability of the received SNR per bit falling in the error-occurable region can be significantly reduced despite of no antenna diversity. Figure 4 shows how antenna diversity reception affects the pdf of γ for the case of $\text{SF} = 32$. It is seen that as the number of antennas increases, the pdf curve shifts to the right owing to the higher average received power.

3.3. BER Performance

The theoretical analysis of the BER performance in the presence of chip interleaving is presented in this section.

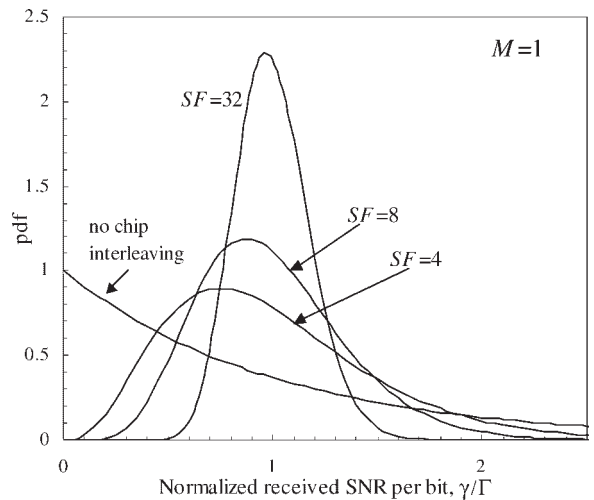


Fig. 3. Theoretical pdf of received signal-to-noise ratio (SNR) per bit with spreading factor (SF) as a parameter for $M = 1$.

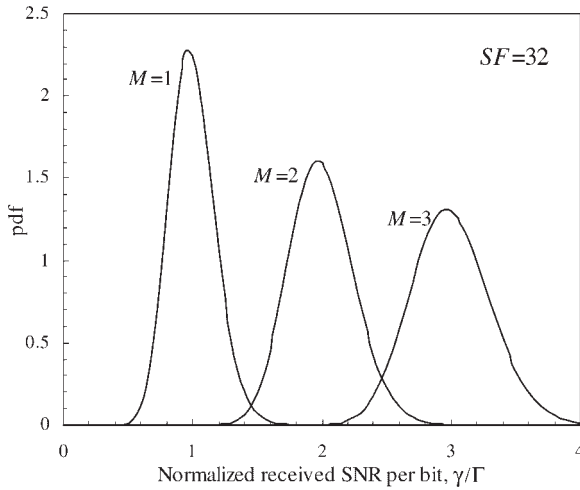


Fig. 4. Theoretical pdf of received SNR per bit with M as a parameter for $SF=32$.

The average BER can be calculated from

$$P_b = \int_0^{\infty} p_b(\gamma)p(\gamma) d\gamma \quad (12)$$

where $p(\gamma)$ is given by Equation (11) and $p_b(\gamma)$ is the conditional error probability given by [2]

$$p_b(\gamma) = \frac{1}{2} \operatorname{erfc} \sqrt{\gamma} \quad (13)$$

for BPSK modulation. Equation (12) has a closed form solution of the form [2]

$$\begin{aligned} P_b &= \left(\frac{1}{2}(1-\mu) \right)^{SF \times M} \\ &\times \sum_{k=0}^{SF \times M - 1} \binom{SF \times M - 1 + k}{k} \left(\frac{1}{2}(1+\mu) \right)^k \quad (14) \\ &\approx \left(\frac{1}{4\bar{\gamma}_c} \right)^{SF \times M} \quad \text{for } \bar{\gamma}_c \gg 1 \end{aligned}$$

where $\mu = \sqrt{\bar{\gamma}_c / (1 + \bar{\gamma}_c)}$. On the other hand, the average BER without both chip interleaving and antenna diversity reception is obtained by letting $SF \times M = 1$ in Equation (14) and is given by

$$\begin{aligned} P_b &= \frac{1}{2} \left[1 - \sqrt{\frac{\Gamma}{1+\Gamma}} \right] \quad (15) \\ &\approx \frac{1}{4\Gamma} \quad \text{for } \Gamma \gg 1 \end{aligned}$$

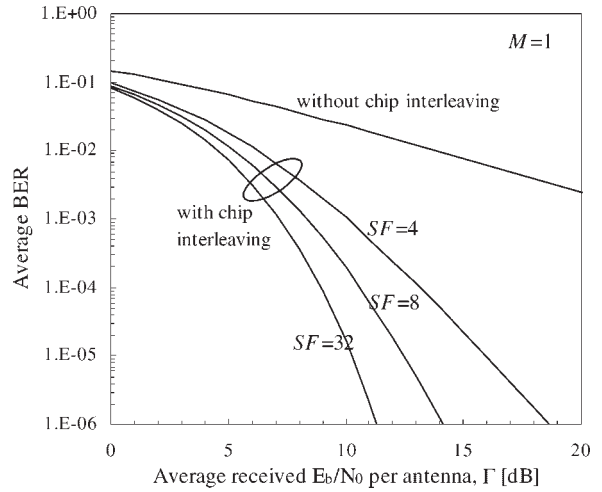


Fig. 5. Theoretical uncoded bit error rate (BER) performance with SF as a parameter for $M=1$.

Figures 5 and 6 plot the theoretical uncoded BER performances as a function of the average received E_b/N_0 per antenna, Γ , with and without chip interleaving. It can be clearly seen in Figure 5 that the use of chip interleaving significantly improves the average BER performance compared to the no chip interleaving case. As the spreading factor becomes larger, the performance improves. This is because the use of chip interleaving is equivalent to using SF -antenna diversity reception (see Equation (14)) but with average E_c/N_0 per antenna reduced by a factor of SF (chip interleaving does not increase the average received signal power). Additional use of antenna diversity

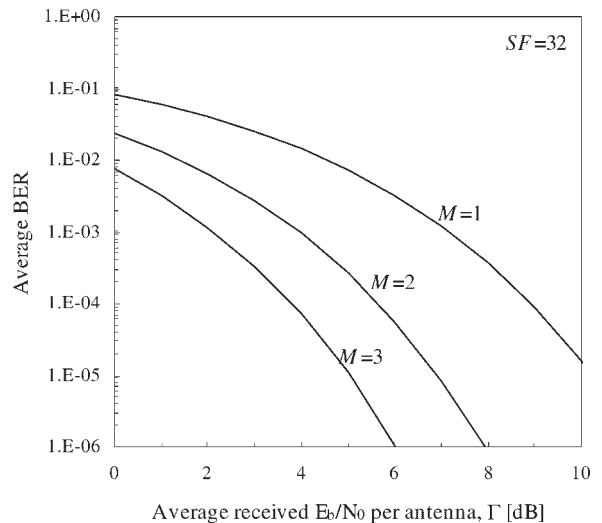


Fig. 6. Theoretical uncoded BER performance with M as a parameter for $SF=32$.

reception can further improve the average BER performance as shown in Figure 6.

4. Computer Simulation

The simulation conditions are summarized in Table I. For the simulation purpose, we consider a rate 1/2 (punctured from rate 1/3) turbo code consisting of two (13,15) recursive systematic encoders with an S-random interleaver [10] between them with $S \approx \sqrt{K}$, where the information sequence length K is taken to be 2^{13} for all cases, except when the effect of K is analyzed. Spreading sequence $\{pn_i\}$ is a pseudo noise (PN)-sequence of period 4096 chips. Pilot-assisted channel estimation is carried out using the weighted multi-slot averaging (WMSA) method [9] with $N_p = 4$ symbols (i.e. $4 \times SF$ pilot chips) and $N_d = 32$ symbols (i.e. $32 \times SF$ data chips). The channel is assumed to be a frequency non-selective slow Rayleigh fading channel. The chip interleaver structure is as shown in Figure 2 and is a (transmit symbol sequence size \times SF)-chip block interleaver. Unless otherwise stated, the chip interleaver size is 16384×32 (or 18432×32) for ideal (or WMSA) channel estimation. The turbo decoder is based on the log-MAP algorithm [11,12].

4.1. Pdf of Bit Energy

Ideal channel estimation is assumed. The pdf of γ normalized by the average E_b/N_0 obtained from computer simulations for the maximum Doppler frequency normalized by the chip length $f_D T_c = 3.1 \times 10^{-5}$ (this corresponds to $f_D T = 1 \times 10^{-3}$, $f_D T = 2.5 \times 10^{-4}$ and $f_D T = 1.25 \times 10^{-4}$ for SF=32, 8 and 4 respectively) and $M = 1$ (no antenna diversity)

Table I. Simulation condition.

Information sequence length	$K = 2^{10} \cdot 2^{13}$ bits	
Turbo coding	Rate	1/2
	Component encoder	(13, 15) RSC
	Interleaver	S-random ($S = K^{1/2}$)
	Component decoder	Log-MAP
	No. of iterations	8
Modulation	BPSK	
Multiple access	DS-CDMA	
	SF=4-32	
Propagation channel	Frequency non-selective Rayleigh fading channel	
Channel estimation	WMSA $k = 2$	

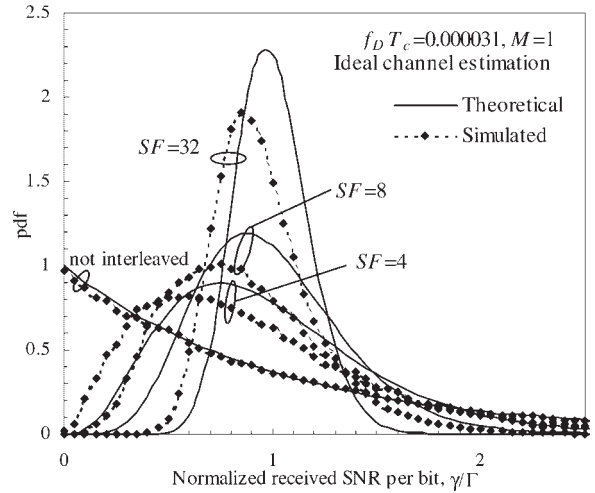


Fig. 7. Simulated pdf of received SNR per bit with SF as a parameter for $M = 1$ and ideal channel estimation.

is plotted in Figure 7, where the dotted lines show the simulation results for $16384 \times SF$ -chip interleaver. For comparison, the theoretical values plotted in Figure 3 are also plotted for reference as solid lines. The pdf of simulation results resembles that of theoretical results but is slightly deviated. The resemblance confirms that the use of chip interleaving is equivalent to using SF-antenna diversity reception but with reduced average E_b/N_0 per antenna by a factor of SF. The deviation of the simulation results from the theoretical value is due to the fact that the channel gains of the chips belonging to the same symbol are partially correlated. The theoretical values are derived under the assumption that the fading experienced by the different chips of the same symbol are independent. Assuming the Jakes model [13], multipath waves arrive at the receive antenna from all directions uniformly and the fading correlation ρ between the adjacent chips of the same bit is given by

$$\begin{aligned} \rho &= J_0 \left(2\pi f_D T_c N \left(1 + \frac{N_p}{N_d} \right) \right) \\ &= J_0 \left(2\pi f_D T \frac{N}{SF} \left(1 + \frac{N_p}{N_d} \right) \right) \end{aligned} \quad (16)$$

For our case, Equation (16) becomes $\rho = J_0((2\pi \times 16384/SF)f_D T)$. As the fading becomes faster, the correlation between the adjacent chips of the same symbol reduces and all the chips tend to experience independent fading; when $f_D T = 0.001$, 0.003 and 0.01, the value of ρ becomes -0.32 , -0.2 and 0.13 respectively. Figure 8 plots the simulated pdf of γ/Γ

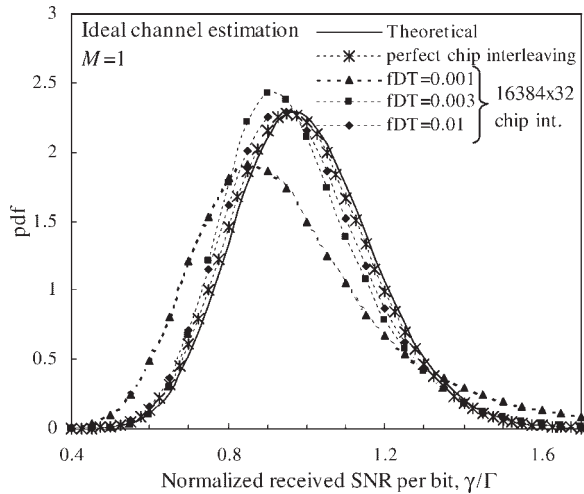


Fig. 8. Simulated pdf of received SNR per bit with $f_D T$ as a parameter for $M=1$, $SF=32$ and ideal channel estimation.

for various values of $f_D T$, while Figure 9 plots the simulated pdf of γ/Γ with the number M of antennas as a parameter. For reference, the simulated pdf curves for perfect chip interleaving (i.e. all the chips experience independent fading) and theoretical ones are also plotted. It is seen from Figure 8 that as the fading becomes faster, the pdf curve becomes closer to the theoretical pdf curve obtained by assuming independent fading. Also, the curves for perfect chip interleaving coincide with the theoretical curves. It is seen from Figure 9 that even when $f_D T=0.001$, the pdf curves for 16384×32 -chip interleaver has a similar form to the theoretical ones for $M=1-3$ (the deviation from theory is due to the residual fading correlation).

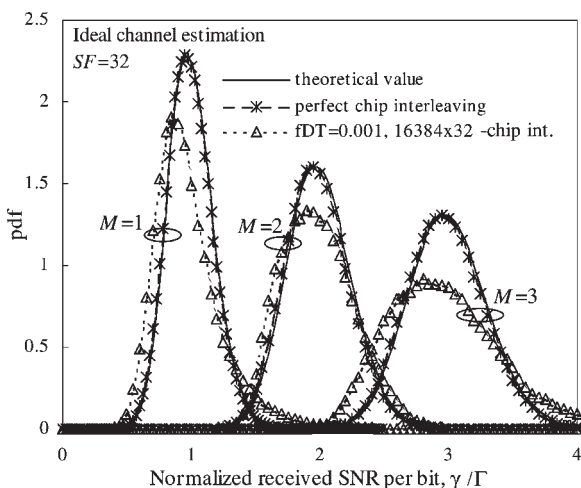


Fig. 9. Simulated pdf of received SNR per bit with M as a parameter for $SF=32$ and ideal channel estimation.

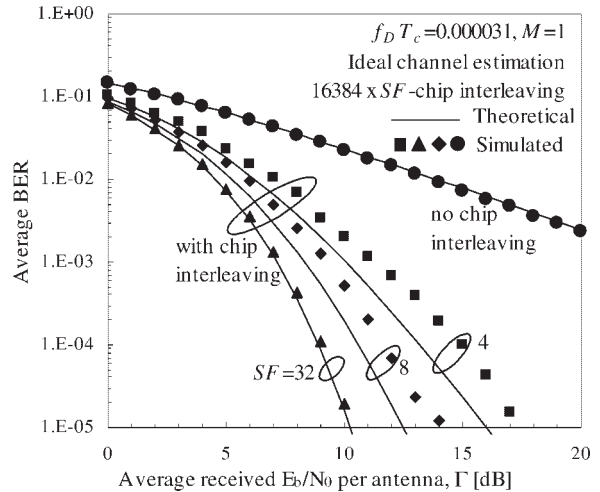


Fig. 10. Simulated uncoded BER performance with SF as a parameter for $M=1$ and ideal channel estimation.

4.2. Chip Interleaving Effect on Uncoded BER Performance

The simulated uncoded BER curves achieved by chip interleaving are plotted in Figures 10 and 11 for $f_D T_c = 0.000031$. For comparison, theoretical uncoded BER curves are also plotted. Ideal channel estimation is assumed. From Figure 10, we see that the simulated curves resemble the theoretical curves and that the BER reduces with increasing SF ; the slight deviation is due to the presence of fading correlation among the chips belonging to the same symbol as discussed in subsection 4.1. The resemblance confirms that the use of chip interleaving is equivalent to using SF antenna

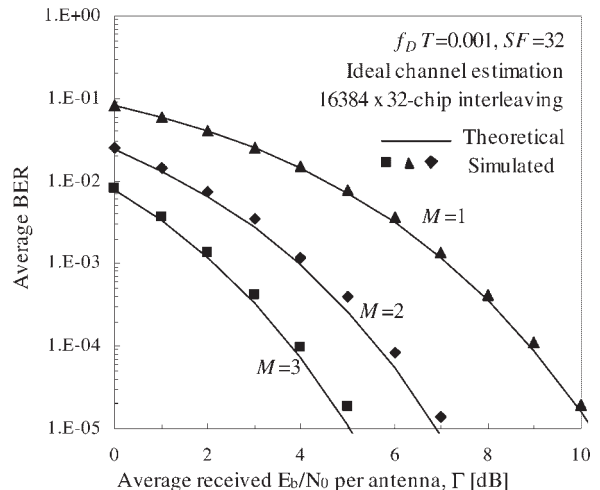


Fig. 11. Simulated uncoded BER performance with M as a parameter for $SF=32$ and ideal channel estimation.

diversity reception for $M = 1$ but with reduced average E_b/N_0 per antenna by a factor of SF. Even in the case of antenna diversity reception, the simulated curves are similar to the theoretical curves as can be seen in Figure 11.

4.3. Combined Effect of Chip Interleaving and Turbo Coding

So far we have presented that chip interleaving can significantly improve the uncoded BER performance. This section evaluates how the BER performance improves when turbo coding is combined with chip interleaving and discusses the effect of various parameters, *viz.* interleaver size, interleaving depth, information sequence length, spreading factor and the fading maximum Doppler frequency.

4.3.1. Chip interleaving gain

Figure 12 plots the coded BER performance for $SF=32$ and $M=1$ as a function of the average received E_b/N_0 per antenna for $K=2^{13}$, which allows the use of 18432×32 -chip interleaving and 128×128 -bit interleaving, both having the same interleaving delay in time. For comparison, the BER performance curves with perfect interleaving and ideal channel estimation (16384×32 -chip interleaver) are also plotted. Let us first concentrate on the BER curves with bit interleaving. It is seen that compared to perfect bit interleaving, the required E_b/N_0 for $BER = 10^{-4}$ degrades by nearly 2.5 dB with an ideal

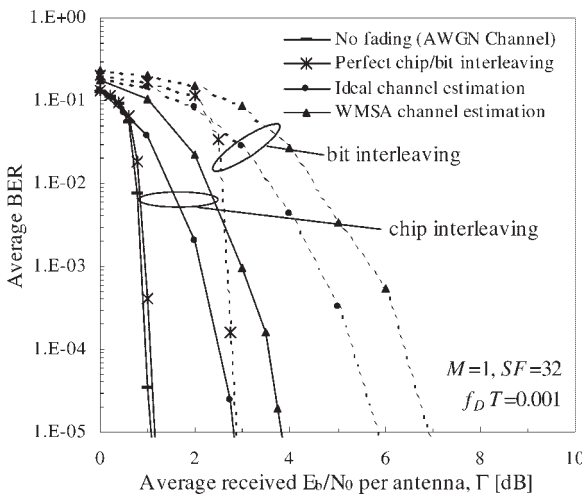


Fig. 12. Simulated coded BER performances with 16384×32 -chip interleaving (solid curves) and with 128×128 -bit interleaving (dashed curves) for $SF=32$ and $M=1$.

cannel estimation. WMSA channel estimation further degrades the performance by 1.5 dB. The solid curves are the BER curves with chip interleaving. The performance is always better than that with bit interleaving. Assuming ideal channel estimation, chip interleaving reduces the required E_b/N_0 for $BER = 10^{-4}$ by nearly 2.6 dB compared to bit interleaving. When WMSA channel estimation is used with chip interleaving instead of bit interleaving, an improvement of 3 dB is obtained. It is interesting to note that the BER performance with chip interleaving and WMSA channel estimation is better than that with bit interleaving and ideal channel estimation.

4.3.2. Impact of chip-interleaver shape

The chip interleaver shown in Figure 2 is a (transmit symbol sequence size \times SF)-chip interleaver. The impact of other interleaver shapes is evaluated here. Figure 13 plots the average BER as a function of the average received E_b/N_0 per antenna with the interleaver shape as a parameter for the information bit sequence length $K=2^{13}$ and $SF=32$. Ideal channel estimation is assumed in order to concentrate on the impact of interleaver shape only. It can be observed from Figure 13 that using a chip interleaver is better than using a 128×128 -bit interleaver. However, the best performance is attained when the chip interleaver shape is 16384×32 . In this case, the chips belonging to a symbol are the furthest possible. The required average received E_b/N_0 is nearly 1 dB less for a $BER = 10^{-4}$ compared to the case when the interleaver is a 4096×128 -chip interleaver. Hence, it can be

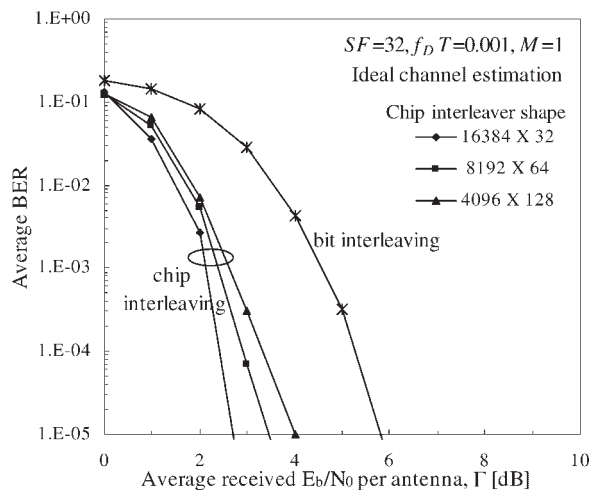


Fig. 13. Impact of chip interleaver shape on coded BER performance for $SF=32$, $M=1$ and ideal channel estimation.

said that the lowest BER is attained for a chip interleaver structure as shown in Figure 2. Henceforth, the chip interleaver shape is always taken as (transmit symbol sequence size \times SF).

4.3.3. Impact of spreading factor

The performance of chip interleaving is dependent on SF. Figure 14 plots the coded BER curves as a function of E_b/N_0 per antenna with SF as parameter for WMSA channel estimation. The $f_D T_c$ value was taken to be $f_D T_c = 0.000031$. The size of the chip interleaver is taken to be (transmit symbol sequence size \times SF) as it is the optimum, where transmit symbol sequence size = 18432 for WMSA channel estimation. The higher the SF for a given $f_D T_c$ value, the better is the BER performance as can be seen from Figure 14. The coded BER performance with chip interleaving is better than that with 128×128 -bit interleaving for all SF. As was mentioned earlier, using a chip interleaver is equivalent to SF-antenna diversity reception. Hence, the fading variations are better removed with higher SF, increasing the diversity effect.

4.3.4. Impact of frame length

Turbo codes are frame length sensitive channel codes. The longer the frame length, the better is the BER performance as the internal interleaver size becomes larger and the allowable bit interleaver also becomes larger. (The bit interleaver used here is a $2^a \times 2^b$ block

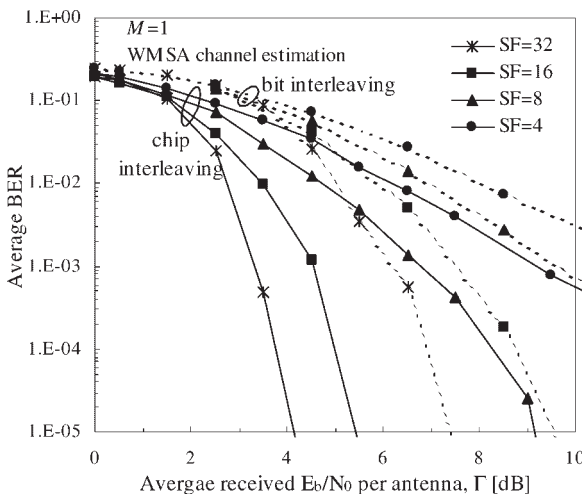


Fig. 14. Impact of spreading factor on coded BER performance with $18432 \times \text{SF}$ -chip (solid lines) and 128×128 -bit (dashed lines) interleaving for $M=1$ and weighted multi-slot averaging (WMSA) channel estimation.

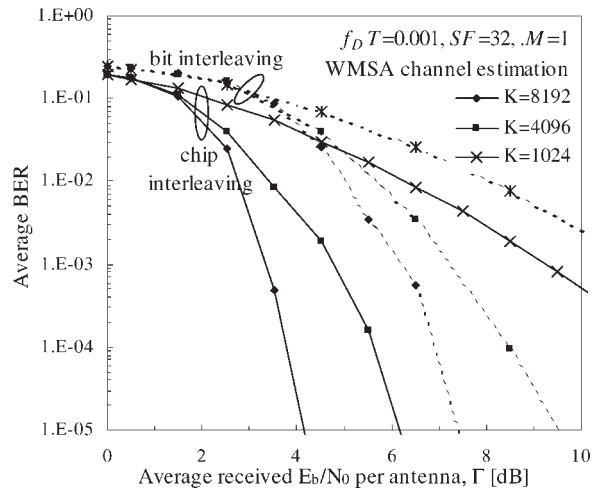


Fig. 15. Impact of frame length on coded BER performance with chip (solid lines) and bit (dashed lines) interleaving for $\text{SF}=32$, $M=1$ and WMSA channel estimation.

interleaver, where a and b are determined so that an interleaver as close as possible to a square interleaver can be obtained.) When chip interleaving is used instead of bit interleaving, similar trend is observed. This can be seen in Figure 15, which plots the coded BER as a function of the average received E_b/N_0 per antenna for different frame lengths and WMSA channel estimation. When $K=8192$, the adjacent chips of a symbol are 18432 chips apart while they are 2304 chips apart when $K=1024$. Thus, the longer the frame length, the less is the correlation among the fading experienced by the chips of the same symbol. The BER after turbo decoding with chip interleaver is better than that with bit interleaving for all values of frame length. The reduction in the required average E_b/N_0 for achieving a $\text{BER} = 10^{-4}$ is 3, 2.6 and 2 dB for $K=8192$, 4096 and 1024 respectively.

4.3.5. Impact of fading rate

Error correction capability of turbo coding varies with the change in the fading rate. For higher maximum Doppler frequency f_D , the interleaving effect improves and hence the coded BER performance becomes better. This can be observed in Figure 16 which plots the coded BER performance with $f_D T$ as a parameter for WMSA channel estimation, $K=2^{13}$ and $\text{SF}=32$. It is seen that the BER performance with chip interleaving (solid lines) is always better than that with bit interleaving (dashed lines). As understood from Figure 8, even for slow fading rate, the pdf curve of the received SNR per bit resembles that of the perfect

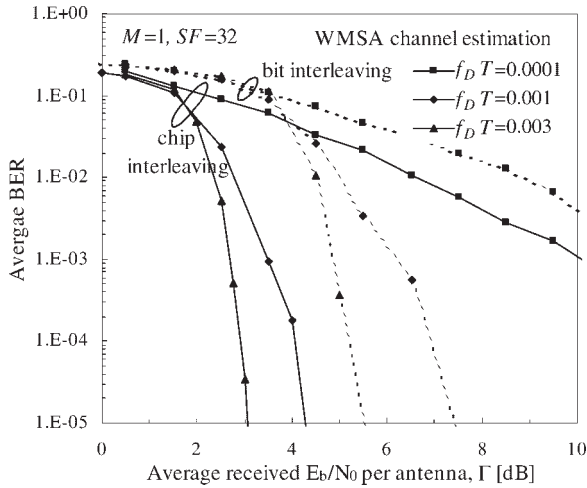


Fig. 16. Impact of fading rate on coded BER performance with 18432×32 -chip (solid lines) and 128×128 -bit (dashed lines) interleaving for $M=1$ and WMSA channel estimation.

chip interleaving. Hence the chip interleaving improvement is present in all cases.

4.3.6. Impact of antenna diversity reception

So far, we assumed a single receive antenna ($M = 1$). In this subsection, the impact of using MRC antenna diversity reception on the achievable coded BER performance with chip interleaving is evaluated.

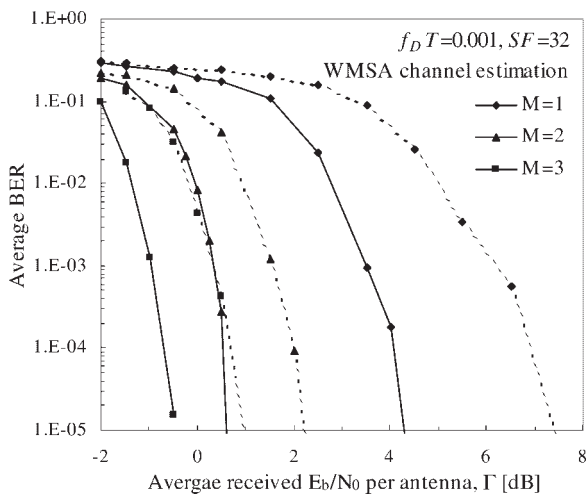


Fig. 17. Impact of antenna diversity on coded BER performance with 18432×32 -chip (solid lines) and 128×128 -bit (dashed lines) interleaving for $SF = 32$ and WMSA channel estimation.

Figure 17 plots the coded BER performances with the number of antennas M as a parameter for WMSA channel estimation, $K = 2^{13}$ and $SF = 32$. The BER performance improves with the increase in the number of antennas (this is also understood from Figure 9). Irrespective of whether chip interleaving or bit interleaving is used, large performance improvements, as a result of antenna diversity, are seen. The performance with 18432×32 -chip interleaving is better than that with 128×128 -bit interleaving for all values of M . However, as M increases, the additional improvement reduces since, with antenna diversity reception, the probability of deep fades is less, so the chip interleaving effect is less.

5. Conclusion

This paper presented a comprehensive performance evaluation of how chip interleaving alters the received signal statistics for DS-SS in a frequency non-selective Rayleigh fading channel with antenna diversity reception. First, the effect of chip interleaving alone was theoretically analyzed assuming an uncoded system. It was confirmed theoretically and by computer simulation that chip interleaving can alter the pdf of the received SNR per bit after despreading in a way similar to antenna diversity reception but with reduced average received signal power by a factor of SF . Then, we evaluated by means of computer simulation the combined effect of chip interleaving and turbo coding and compared to the case of conventional bit interleaving. It was shown that the best performance is obtained when the chip interleaver size is (transmit symbol sequence size $\times SF$) and that the coded BER performance improves when chip interleaving is used instead of bit interleaving. It was also found that the coded BER performance improves with increasing SF and increasing frame length. Chip interleaving was found effective in the presence of antenna diversity reception as well.

In this paper, the analysis has been done for a frequency non-selective Rayleigh fading channel. In a frequency selective fading channel, rake combining can be used to improve the BER performance. For a large spreading factor, rake combining is equivalent to antenna diversity reception with the number of antennas equal to the number of propagation paths. Therefore, the results obtained in this paper can also be applied to DS-SS using rake combining in a frequency selective fading channel. Recently multicarrier DS-CDMA [14] is being considered for uplink transmission

as it has the desirable properties of exhibiting a narrowband interference suppression effect, along with robustness to fading, without requiring the use of either an explicit rake structure or an interference suppression filter. The channel for each carrier is a narrowband frequency non-selective channel. The evaluations done in this paper can be applied for each carrier in a multicarrier DS-CDMA system as well.

References

1. Adachi F, Sawahashi M, Suda H. Wideband DS-CDMA for next generation mobile communications systems. *IEEE Communications Magazine* 1998; **36**(9): 56–69.
2. Proakis JG. *Digital Communications*. McGraw Hill: Singapore, 2001.
3. Diaz P, Agusti R. The use of coding and diversity combining for mitigating fading effects in a DS/CDMA system. *IEEE Transactions on Vehicular Technology* 1998; **47**(1): 95–102.
4. Berrou C, Glavieux A. Near optimum error correcting coding and decoding: turbo codes. *IEEE Transactions on Communications* 1996; **44**(10): 1261–1271.
5. Garg D, Adachi F. Chip interleaved turbo codes for DS-CDMA mobile radio in a fading channel. *Electronics Letters* 2002; **38**(13): 642–643.
6. Cirpan HA, Tsatsanis MK. Chip interleaving in direct sequence CDMA systems. In *Proceedings of ICASSP* 1997; pp. 3877–3880.
7. Zhou S, Giannakis GB, LeMartret C. Chip-interleaved block-spread code division multiple access. *IEEE Transactions on Communications* 2002; **50**(2): 235–248.
8. Lin YN, Lin DW. Multiple access over fading multipath channels employing chip-interleaving code-division direct-sequence spread spectrum. *IEICE Transactions on Communications* 2003; **E86-B**(1): 114–121.
9. Andoh H, Sawahashi M, Adachi F. Channel estimation filter using time-multiplexed pilot channel for coherent RAKE combining in DS-CDMA mobile radio. *IEICE Transactions on Communications* 1998; **E81-B**(7): 1517–1526.
10. Divsalar D, Pollara F. Turbo-codes for PCS applications. In *Proceedings of ICC* 1995; pp. 54–59.
11. Woodard JP, Hanzo L. Comparative study of turbo decoding techniques: an overview. *IEEE Transactions on Vehicular Technology* 2000; **49**(6): 2208–2233.
12. Robertson P, Villebrum E, Hoeher P. A comparison of optimal and sub-optimal MAP decoding algorithms operating in the log domain. In *Proceeding of ICC* 1995; pp. 1009–1013.
13. Jakes WC, Jr. *Microwave Mobile Communications*. Wiley: New York, 1974.
14. Hara S, Prasad R. Overview of multicarrier CDMA. *IEEE Communications Magazine* 1997; **32**(12): 126–133.

Authors' Biographies



Deepshikha Garg received her B.E. degree in electrical and communications engineering from Kathmandu University, Nepal in 1998. Currently she is in the Ph.D. program in the Department of Electrical and Communications Engineering at Tohoku University, Sendai, Japan. Her research interests include error control schemes and accessing techniques for wireless communications. She was the recipient of the 2002 active research award in radio communication systems from IEICE in 2002.



Fumiuyuki Adachi received his B.S. and Dr.Eng. degrees in electrical engineering from Tohoku University, Sendai, Japan, in 1973 and 1984 respectively. In April 1973, he joined the Electrical Communications Laboratories of Nippon Telegraph & Telephone Corporation (now NTT) and conducted various types of research related to digital cellular mobile communications. From July 1992 to December 1999, he was with NTT Mobile Communications Network, Inc. (now NTT DoCoMo, Inc.), where he led a research group on wideband/broadband CDMA wireless access for IMT-2000 and beyond. Since January 2000, he has been with Tohoku University, Sendai, Japan, where he is a professor of electrical and communication engineering at Graduate School of Engineering. His research interests are in CDMA and TDMA wireless access techniques, CDMA spreading code design, Rake receiver, transmit/receive antenna diversity, adaptive antenna array, bandwidth-efficient digital modulation, and channel coding, with particular application to broadband wireless communications systems. From October 1984 to September 1985, he was a United Kingdom SERC visiting research fellow in the Department of Electrical Engineering and Electronics at Liverpool University. From April 1997 to March 2000, he was a visiting professor at Nara Institute of Science and Technology, Japan. He was a recipient of IEICE Achievement Award 2002 and was a co-recipient of the IEICE Transactions best paper of the year award 1996 and again 1998. He is an IEEE fellow and was a co-recipient of the IEEE Vehicular Technology Transactions best paper of the year award 1980 and again 1990 and also a recipient of Avant Garde award 2000.